Predictive data-based exposition of $5s5p\ ^{1,3}P_1$ lifetimes in the Cd isoelectronic sequence

L. J. Curtis,[1,*] R. Matulioniene,[2] D. G. Ellis,[1] and C. Froese Fischer[2]
[1]*Department of Physics and Astronomy, University of Toledo, Toledo, Ohio 43606*
[2]*Department of Computer Science, Vanderbilt University, Nashville, Tennessee 37235*
(Received 18 July 2000; published 16 October 2000)

Experimental and theoretical values for the lifetimes of the $5s5p\ ^1P_1$ and $^3P_1$ levels in the Cd isoelectronic sequence are examined in the context of a data-based isoelectronic systematization. Lifetime and energy-level data are combined to account for the effects of intermediate coupling, thereby reducing the data to a regular and slowly varying parametric mapping. This empirically characterizes small contributions due to spin-other-orbit interaction, spin dependences of the radial wave functions, and configuration interaction, and yields accurate interpolative and extrapolative predictions. Multiconfiguration Dirac-Hartree-Fock calculations are used to verify the regularity of these trends, and to examine the extent to which they can be extrapolated to high nuclear charge.

PACS number(s): 32.70.Cs, 32.30.Jc

I. INTRODUCTION

Recent comprehensive studies of experimental and theoretical values for the lifetimes of ns^2-$nsnp$ resonance and intercombination transitions in the Be [1], Mg [2], and Zn [3] isoelectronic sequences (as well as preliminary studies of the Cd [4] and Hg [4,5] sequences) have revealed useful predictive regularities. A parametric reduction has been formulated that uses spectroscopic energy-level data to remove the effects of intermediate coupling from measured line strength data. This permits the transition probabilities of both the resonance and intercombination transitions to be accurately predicted through many stages of ionization on the basis of a few accurate measurements near the neutral end of the isoelectronic sequence.

Here we extend and refine this formulation through application to the Cd isoelectronic sequence, using a generalization of the method that includes not only exchange and spin-orbit effects, but also spin-other-orbit interaction and differences between the singlet and triplet radial wave functions. Multiconfiguration Dirac-Hartree-Fock (MCDHF) theoretical calculations [6] have also been made to test the rigor of the linearities that have been exhibited empirically.

The semiempirical (SE) formulation used here parametrizes the effects of intermediate coupling by combining energy-level and lifetime data in an exposition that exhibits a smooth and slowly varying isoelectronic variation. This regularity allows inconsistent measurements to be exposed and eliminated, and data for the entire sequence to be statistically combined through weighted least-squares fitting procedures. In this manner, interpolative and extrapolative predictions are made that can be more accurate than the individual measured values.

II. SEMIEMPIRICAL FORMULATION

The $nsnp$ configuration consists of four levels, denoted here by the standard LS coupling spectroscopic symbols $^3P_2$, $^3P_1$, $^1P_1$, and $^3P_0$. For a pure $nsnp$ configuration in intermediate coupling, the wave functions can be written in terms of two normalized singlet-triplet mixing amplitudes that can be characterized by a single parameter, the singlet-triplet mixing angle θ. This quantity specifies the splittings among the four $nsnp$ energy levels, the lifetimes of the two $nsnp$ $J=1$ levels, and the magnetic g factors of the $J>0$ levels. Under these conditions, the physical $J=1$ levels can be described by the wave functions

$$|^3P_1'\rangle = |^3P_1\rangle \cos\theta - |^1P_1\rangle \sin\theta, \tag{1}$$

$$|^1P_1'\rangle = |^3P_1\rangle \sin\theta + |^1P_1\rangle \cos\theta. \tag{2}$$

The primes indicate the fact that the LS notation for the physical states is only nominal.

A. Mixing angles deduced from energy-level data

The physical energy levels are specified by the Slater parameters E_0 (the electron-nucleus and direct electron-electron energies), G_1 (the exchange electron-electron energy), and μ_1 and μ_2 (the diagonal and off-diagonal magnetic energies) through the relationships [7] (with the measured energy levels denoted here by their spectroscopic symbols)

$$^3P_2 = E_0 - G_1 + \mu_1/2, \tag{3}$$

$$^1P_1', ^3P_1' = E_0 - \mu_1/4 \pm \Delta, \tag{4}$$

$$^3P_0 = E_0 - G_1 - \mu_1, \tag{5}$$

where

$$\Delta \equiv \sqrt{(G_1 + \mu_1/4)^2 + \mu_2^2/2}. \tag{6}$$

The mixing angle can be expressed in terms of G_1, μ_1, and μ_2 as [7,8]

$$\cot 2\theta = (4G_1 + \mu_1)/\sqrt{8}\mu_2. \tag{7}$$

*Electronic address: ljc@physics.utoledo.edu

In the simplest formulation [7,8], the diagonal and off-diagonal magnetic parameters are both set equal to the standard spin-own-orbit energy $\zeta=\mu_1=\mu_2$. However, it has been shown [7,9–11] that allowing μ_1 and μ_2 to vary separately generalizes the parametrization to include the effects of both the spin-other-orbit interaction energy (as first proposed by Wolfe in 1932 [10]) and slight differences between the radial wave functions for the singlet and triplet states (as first proposed by King and Van Vleck in 1939 [11]).

The three parameters G_1, μ_1, and μ_2 comprise an equivalent recharacterization of the measured spectroscopic data, since they are uniquely specified by the measured energy-level data for any three independent level splittings, e.g.,

$$a\equiv {}^1P_1'-{}^3P_1', \tag{8}$$

$$b\equiv {}^3P_2-{}^3P_1', \tag{9}$$

$$c\equiv {}^3P_2-{}^3P_0 \tag{10}$$

of the four levels. It can be seen from Eqs. (3)–(6) that the remapping is given by

$$G_1=(a-2b+c)/2, \tag{11}$$

$$\mu_1=2c/3, \tag{12}$$

$$\mu_2=\sqrt{2(b-2c/3)(a-b+2c/3)}. \tag{13}$$

An empirical fitting function of the form

$$\cot 2\theta\cong D+E/(Z-C)^p \tag{14}$$

has been found [12] to accurately describe the isoelectronic variation of the mixing angles for the Be, Mg, Zn, Cd, and Hg sequences. Here D, E, and C are least-squares adjusted fitting constants. The power law yields $p\cong 1$ for the Zn, Cd, and Hg sequences, and $p>1$ for the Be and Mg sequences, and the fitted value of C is close to the number N of closed core electrons ($N=46$ here). In the simplest formulation where the diagonal and off-diagonal magnetic energies μ_1 and μ_2 are equated, they cancel as they become large compared to the electrostatic exchange energy G_1 for large Z, and Eq. (7) yields $D\rightarrow 1/\sqrt{8}$. Since μ_1 and μ_2 here are allowed to vary freely, the quantity D will be left as a fitting parameter.

B. Reduced line strengths deduced from lifetime data

The line strengths for these unbranched $J=0-1$ transitions can be deduced from the measured lifetimes τ and wavelengths λ using

$$S=3[\lambda(\text{Å})/1265.38]^3/\tau(\text{ns}). \tag{15}$$

For the singlet-singlet resonance (Res) and singlet-triplet intercombination (Int) transitions these quantities can be freed of the effects of singlet-triplet mixing by defining the reduced line strengths S_r

$$S_r(\text{Res})\equiv S(\text{Res})/\cos^2\theta, \tag{16}$$

$$S_r(\text{Int})\equiv S(\text{Int})/\sin^2\theta, \tag{17}$$

which, in the nonrelativistic approximation, involve only factors of the radial matrix elements. Empirically, it has been found that the isoelectronic behavior of these quantities is often accurately represented by the fitting function

$$Z^2S_r\cong S_0+B/(Z-C), \tag{18}$$

where Z is the nuclear charge, and S_0, B, and C are least-squares adjusted fitting constants. For the Mg, Zn, and Hg sequences, it has been observed that the fitted value of quantity S_0 (the asymptotic value of the reduced line strength for infinite Z) is often very close to the corresponding nonrelativistic hydrogenic value [13] (with a factor 2 for the equivalent electrons in the ground state)

$$S_H\rightarrow 9n^2(n^2-1)/2. \tag{19}$$

For the Cd sequence with $n=5$, this yields $S_H=2700$. Similarly, the fitted value of C has been found to be approximately equal to the number of core electrons N beneath the valence shell, which for the Cd sequence is $N=46$.

III. THEORETICAL CALCULATIONS

Ab initio theoretical calculations can provide a useful test of the persistence to higher Z of the regularities in this parameterization exhibited by the existing data base. With increasing ionicity, the behavior of the Cd isoelectronic sequence [14] will be increasingly affected by configuration interaction and relativistic effects. MCDHF calculations introduce both additional configurations and the possibility of a significant dependence upon J of the radial transition elements, and can reveal whether these effects can be adequately characterized by the effective values for the mixing angles and reduced line strengths deduced from this parameterization.

However, there are also limitations to this approach, since the MCDHF code treats contributions important at very high Z (e.g., the Breit interaction and quantum electrodynamic corrections) only perturbatively. Thus the ''infinite-Z limit'' should be regarded only as a useful fiducial point for extrapolation of low-Z results to high intermediate values for Z, and not as an actual prediction for the behavior at very high Z.

In a recent theoretical study [15] of the Cd isoelectronic sequence, Biémont *et al.* used the MCDHF method to compute the oscillator strengths for the resonance and intercombination transitions in the Z range 48–57. The present work extends the study of Ref. [15] to higher values of nuclear charge, and focuses on the qualitative isoelectronic trends

TABLE I. Data base of the energy level[a] (in cm^{-1}) and lifetime (in ns) measurements. Parentheses denote quoted uncertainties in the experimental lifetimes.

Z ion	$^3P_0$	$^3P_1$	$^3P_2$	$^1P_1$	τ_{res}	τ_{int}
48 Cd	30 114.02	30 657.13	31 827	43 692.47	1.66(5)[b]	2390(40)[c]
49 In	42 275	43 349	45 827	63 033.81	0.79(5)[d]	440(40)[e]
50 Sn	53 548	55 196.4	59 228.6	79 911.3	0.47(3)[f]	
51 Sb	64 435	66 700	72 560	95 952	0.38(4)[g]	
52 Te	75 110.4	78 025	86 006.3	111 708	0.275(20)[h], 0.260(25)[i]	40(10)[i]
53 I	85 666	89 262	99 686	127 424	0.215(12)[j], 0.25(3)[k]	24.4(12)[k]
54 Xe	96 139.7	100 451.5	113 674.1	143 260.9	0.15(1)[h], 0.18(1)[l]	14.0(7)[l]
55 Cs	106 573	111 631	128 032	159 327		
56 Ba	116 991	122 812	142 812	175 711		
57 La	127 392	134 019	158 052	192 481		

[a]Energy-level data for $Z=48-53$ are from sources quoted in Ref. [14] and those for $Z=54-57$ are from Ref. [16].
[b]Lurio and Novick [17].
[c]Reference [18].
[d]Ansbacher *et al.* [19].
[e]Reference [20]
[f]Reference [21]
[g]Pinnington *et al.* [22].
[h]Pinnington *et al.* [23].
[i]Pinnington *et al.* [24].
[j]Ansbacher *et al.* [25].
[k]O' Neill *et al.* [26].
[l]Kernahan *et al.* [27].

rather than the quantitative predictions of oscillator strengths.

The multiconfiguration expansion was designed to qualitatively capture both valence and core-valence correlation ($V+CV$) effects. For the even-parity states, the expansion was obtained by single and double excitations of the electrons from the reference set $\{4d^{10}5s^2,4d^{10}5p^2,4d^{10}5d^2 J=0\}$ to an active set of orbitals $\{5s,5p,5d,s,p,f,g\}$, with the constraint of creating at most one hole in the $4d$ subshell. The expansion for the odd-parity states was generated in a similar manner, starting with the reference set $\{4d^{10}5s5p,4d^{10}5p5d J=0,1,2\}$, and using the same active set of orbitals as in the case of the even-parity states. The resulting multiconfiguration expansion contained 468 even-parity relativistic configuration state functions (CSFs) of total angular momentum $J=0$, and 3553 odd-parity CSFs with $J=0$, 1, and 2.

The radial orbitals were generated using the optimal level model. The even-parity level selected for targeting had $5s^2$ as its dominant eigenvector component. The odd-parity states were treated using the extended optimal level model; four levels (one $J=0$, two $J=1$, and one $J=2$) were targeted under the requirement that the dominant eigenvector component of each selected level be the (nonrelativistic) CSF $5s5p$. All four levels were assigned equal weights in the energy functional. All the spectroscopic radial orbitals and the $5d$ correlation orbitals were determined by simultaneous optimization in a smaller valence-correlation calculation that included the even-parity $J=0$ levels of $\{5s^2,5p^2,5d^2\}$, and the odd-parity $J=0,1,2$ levels of $\{5s5p,5p5d\}$. In the $V+CV$ calculation, the orbitals up to $5d$ were taken from this smaller calculation, and kept frozen in the variational procedure to determine the correlation orbitals *s,p,f,g*.

IV. DATA SOURCES

The energy-level data base is listed in Table I. These values were taken for $Z=48-53$ from the primary sources quoted in Ref. [14], and for $Z=54-57$ from the measurements of Kaufman and Sugar [16]. For extrapolative predictions of the transition wavelengths for $Z\geqslant 58$ the values given in Ref. [14] (which are based on a combination of semiempirical and *ab initio* methods) were used.

A critical selection was made of the lifetime data [17–27]. It is well known that some of the early lifetime measurements made for charged ions by curve fitting methods (prior to the development of the cascade-correlated analysis of decay curves method [28,29]) were distorted by cascade repopulation [29]. Since these early measurements have now been repeated using methods that take cascade repopulation into account, we have excluded all measurements for charged ions made prior to 1974 from our compilation [30–32]. In the case of neutral Cd, we have selected measurements utilizing the Hanle effect to determine the resonance transition [17] and optical double resonance methods to determine the intercombination transition [18]. These 1963 measurements quote accuracies of 3% and 1.7%. The measurements selected for inclusion in this analysis are listed in

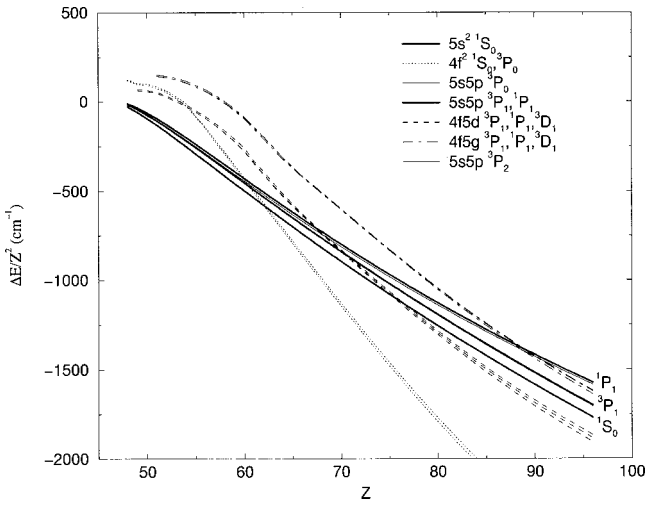

FIG. 1. Energies relative to $4d^{10}5s\ ^2S_{1/2}$, with valence correlation only. Many more crossings occur in the $(CV+V)$ calculation at high Z, as the f correlation orbital becomes the spectroscopic $4f$ in CSF's such as $4d^9 4f 5\{s,p,d\}nl$, $4d^9 4f^2 5\{s,p,d\}$.

Table I, together with their quoted uncertainties. For purposes of plotting, a weighted average was taken in cases where multiple measurements exist.

V. RESULTS

A. Energy levels and mixing angles

The results of the calculations for the energies relative to the $4d^{10}5s\ ^2S_{1/2}$ ground state, done using valence correlation only, are presented in Fig. 1. As the nuclear charge increases, plunging configurations that involve $4f$ orbitals cross the levels of interest. For $Z>62$ the $4f^2$ levels become the ground configuration, so this becomes a transition between core excited states [16]. For $Z=67-71$, plunging levels from the $4f5d$ configuration complicate the interpretation though extensive configuration interaction, and thereafter levels from this configuration provide additional decay channels that cause the lifetime to differ from the reciprocal of these transition probabilities.

The experimental energy level data base for the $5s5p$ levels is given in Table I. These values, together with the extrapolations of Ref. [14], and the theoretical calculations

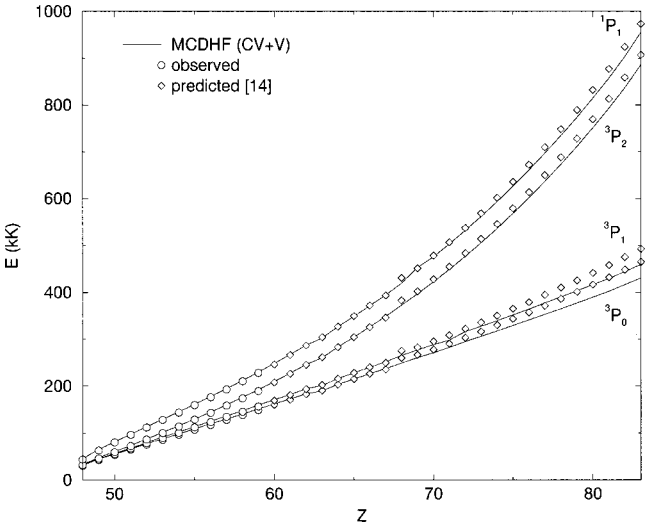

FIG. 2. Theoretical, experimental, and semiempirical values for the $5s^2\ ^1S_0-5s5p\ ^{1,3}P_1$ energy intervals. Solid lines indicate MCDHF$(CV+V)$ calculations, O denotes observed values, and ◇ indicates the semiempirical extrapolations of Ref. [14].

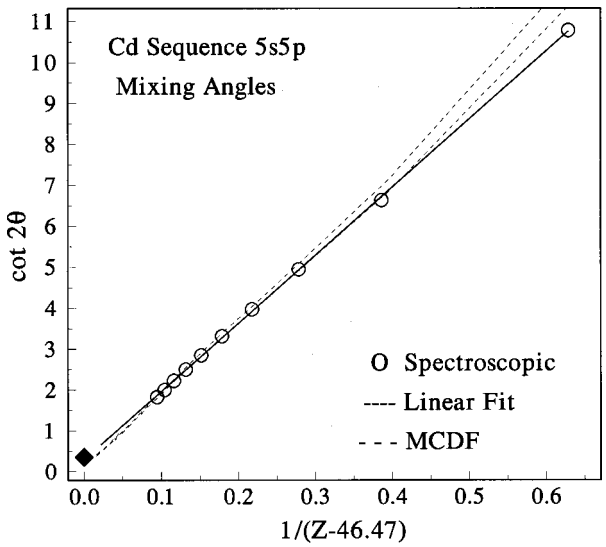

FIG. 3. Isoelectronic exposition of $\cot 2\theta$. The symbol O denotes the values obtained from the experimental energy levels using Eqs. (7)–(13), and the solid line is a fit to these values. The dashed curves trace the amplitudes obtained from the MCDHF calculations for the singlet (lower curve) and triplet (upper curve) configuration state vectors. The symbol ◇ denotes the *jj* limit.

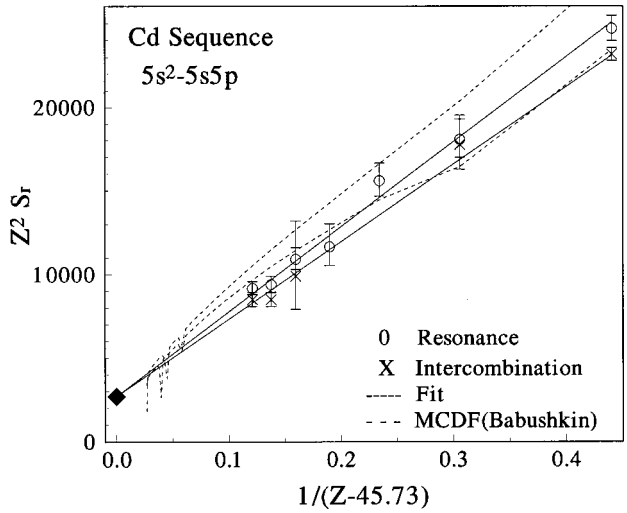

FIG. 4. Reduction of the lifetime data for the Cd sequence. Measured values and source references are given in Table I. The symbols *O* and × denote the values for the reduced line strengths of resonance and intercombination transitions obtained from measured data in Eqs. (7)–(16). The solid lines are fits to the measured data, and the dashed curves are reductions of the MCDHF calculations made here. The symbol ◇ denotes the hydrogenic value.

TABLE II. Results for the resonance transition $5s^2\ ^1S_0-5s5p\ ^1P_1$. Parentheses indicate quoted uncertainties in the experimental values as propagated from Table I.

		A_{ik} (ns^{-1})					
			MCDHF[a]		MCDHF[b]		
Z ion	λ (Å)	Expt.	Coulomb	Babushkin	Coulomb	Babushkin	SE[c]
48 Cd	2289	0.602(18)	0.595	0.617	0.752	0.773	0.611
49 In	1586	1.27(8)	1.36	1.38	1.54	1.58	1.28
50 Sn	1251	2.13(14)	2.22	2.22	2.42	2.39	1.99
51 Sb	1042	2.63(28)	3.19	3.18	3.39	3.33	2.78
52 Te	895	3.72(22)	4.31	4.27	4.58	4.49	3.67
53 I	785	4.55(23)	5.55	5.49	5.86	5.75	4.67
54 Xe	698	6.02(25)	6.94	6.85	7.29	7.14	5.80
55 Cs	628		8.47	8.33	8.86	8.68	7.06
56 Ba	569		10.2	10.0	10.6	10.4	8.46
57 La	520		12.0	11.9	12.5	12.3	10.0
58 Ce	477				14.6	14.3	11.8
59 Pr	439				16.9	16.6	13.8
60 Nd	406				19.4	19.1	16.1
61 Pm	377				22.1	21.8	18.6
62 Sm	349				24.5	24.8	21.6
63 Eu	329				22.4	24.0	24.1
64 Gd	306				30.0	31.1	27.9
65 Tb	287				34.8	35.3	31.9
66 Dy	269				39.5	39.5	36.3
67 Ho	254				44.2	43.7	40.5

[a]Biémont *et al.* [15].

[b]This work, theoretical.

[c]This work, semiempirical, from fits shown in Figs. 3 and 4 and Eqs.(20) and (22).

made here are shown in Fig. 2. The agreement between theory and experiment is close for low to intermediate values of Z, with a tendency for the theoretical values to fall slightly below the semiempirical extrapolations for $Z>67$, where the formulation is affected by plunging levels.

The measured base of energy level data was used to specify the mixing angles through the use of Eqs. (7)–(13). These mixing angles were then isoelectronically parameterized through the least-squares adjustment of Eq. (14) (setting $p\equiv 1$) to obtain $D=0.298$ (slightly less than $1/\sqrt{8}=0.3535...$), $C=46.41$, and $E=16.628$. A plot of $\cot 2\theta$ vs $1/(Z-C)$ is presented in Fig. 3, indicating the measured data, the least-squares fit, and the amplitudes obtained from the MCDHF calculation. This fit was used to interpolate and extrapolate the values of the mixing angle along the isoelectronic sequence. Note that for $Z>60$ the MCDHF values also fall below the trend toward the nonrelativistic asymptotic value of $1/\sqrt{8}$.

In forming the values for the reduced line strengths of the multiconfiguration theoretical calculations, the existence of more than two $J=1$ basis states requires that the mixing angles be replaced by mixing amplitudes. Thus two separate mixing angles were defined, $\cos\theta_1$ and $\sin\theta_3$, corresponding respectively to the amplitudes of the $^1P_1$ basis state in upper (nominally $^1P_1$) and lower (nominally $^3P_1$) $J=1$ configuration state vectors considered. Here $\cos^2\theta_1+\sin^2\theta_3$ does not necessarily yield unity, and its value indicates the degree to which other configurations enter the calculation.

B. Lifetimes and line strengths

The critically chosen experimental lifetime measurements and wavelength data in Table I were inserted into Eq. (15) to obtain the line strengths S, and then combined with mixing angle data using Eqs. (16) and (17) to obtain the reduced line strengths S_r. These values are scaled by Z^2 and plotted vs $1/(Z-C)$ in Fig. 4, which also displays reductions of the theoretical calculations presented here.

The use of the Wolfe method [10], in which μ_1 and μ_2 are allowed to vary separately as independent fitting parameters, made a marked improvement in the representation of the intercombination transition for the neutral and singly ionized members of the sequence. The use of three fitting parameters yielded a somewhat smaller value for the effective singlet-triplet mixing angle than that obtained using only two fitting parameters. This significantly improved the fit for the intercombination transitions in the region where $\sin\theta\leqslant 0.1$.

Weighted least-squares adjustments of these data to Eq. (18) were made. These indicated that the value of the high-Z intercept could be well represented by $S_0=S_H$. Moreover, it was found that both the resonance and intercombination tran-

TABLE III. Results for the intercombination transition $5s^2\ ^1S_0-5s5p\ ^3P_1$. Parentheses indicate quoted uncertainties in the experimental values as propagated from Table I.

		A_{ik} (ns^{-1})					
			MCDHF[a]		MCDHF[b]		
Z ion	λ (Å)	Expt.	Coulomb	Babushkin	Coulomb	Babushkin	SE[c]
48 Cd	3262	0.000418(7)	0.000348	0.000343	0.000449	0.000356	0.000419
49 In	2307	0.0023(2)	0.00212	0.00197	0.00244	0.00210	0.00210
50 Sn	1812		0.00676	0.00606	0.00701	0.00649	0.00614
51 Sb	1499		0.0154	0.0142	0.0158	0.0147	0.0137
52 Te	1282	0.025(6)	0.0304	0.0279	0.0310	0.0290	0.0261
53 I	1120	0.041(2)	0.0535	0.0490	0.0539	0.0509	0.0445
54 Xe	966	0.071(4)	0.0862	0.0793	0.0868	0.0822	0.0702
55 Cs	896		0.132	0.120	0.131	0.125	0.104
56 Ba	814		0.189	0.175	0.189	0.180	0.148
57 La	746		0.256	0.256	0.263	0.251	0.202
58 Ce	688				0.352	0.337	0.268
59 Pr	637				0.460	0.441	0.346
60 Nd	593				0.586	0.563	0.439
61 Pm	554				0.730	0.705	0.547
62 Sm	518				0.866	0.860	0.677
63 Eu	494				0.789	0.869	0.781
64 Gd	465				1.17	1.21	0.950
65 Tb	439				1.45	1.45	1.12
66 Dy	417				1.73	1.70	1.31
67 Ho	401				2.04	1.96	1.47

[a]Biémont *et al.* [15].
[b]This work, theoretical.
[c]This work, semiempirical, from fits shown in Figs. 3 and 4 and Eqs. (21) and (22).

sition data could be effectively linearized by the same value of C. Therefore the fits, subject to constraints $S_0=2700$ and $C(\mathrm{Res})=C(\mathrm{Int})$, yielded $C=45.73$, $B(\mathrm{Res})=50709$, and $B(\mathrm{Int})=46274$. Summarizing, the predicted line strengths can be specified by

$$S(\mathrm{Res})=\left(2700+\frac{50\,709}{Z-45.73}\right)\left(\frac{\cos\theta}{Z}\right)^2, \tag{20}$$

$$S(\mathrm{Int})=\left(2700+\frac{46\,274}{Z-45.73}\right)\left(\frac{\sin\theta}{Z}\right)^2, \tag{21}$$

$$\cot 2\theta=0.298+16.628/(Z-46.41). \tag{22}$$

The fitting constants can subsequently be sharpened as additional lifetime and energy level measurements become available. However it is significant to note that Eqs. (20)–(22) summarize, in very economical form, all of the information that is presently known concerning the line strengths of these Cd-like transitions.

The resonance and intercombination transition probability rates predicted by this semiempirical linearization are tabulated in Tables II and III for $48\leqslant Z\leqslant 67$, together with the wavelengths and the MCDHF calculations. For $Z>50$, the results of the present calculation agree with the predictions of the considerably more elaborate theoretical model of Ref. [15]. This agreement indicates that the present approach should be sufficient to characterize the isoelectronic trends predicted by the MCDHF method at intermediate values of Z; that is, away from the neutral-Z region that is complicated by extensive electron correlation effects, not yet in the high-Z region that is complicated by configuration interaction resulting from level crossings due to the contraction of the $4f$ shell. Although the quantitative description of the high-Z region would require a considerably more thorough theoretical effort, sharp deviations of our theoretical results from the smooth semiempirical isoelectronic trend in the high-Z region indicate the possible breakdown of the semiempirical formulation based on the single-configuration approach.

VI. CONCLUSIONS

The approximate linearities observed in the measured data through their expositions as $\cot 2\theta$ and Z^2S_r vs $1/(Z-C)$ (with C optimally chosen) have been verified for the Cd sequence by MCDHF calculations in the region $48\leqslant Z\leqslant 67$. This confirms the suggestion [4] that a few accurate lifetime measurements for the $5s5p\ ^1P_1$ and $5s5p\ ^3P_1$ levels can be

used to make accurate interpolative, extrapolative, and isoelectronically smoothed predictions for the $5s^2\ ^1S_0 - 5s5p\ ^{1,3}P_1$ transition probability rates for all members of the sequence with $Z \leqslant 67$. For higher values of Z, plunging levels and additional decay channels complicate the situation, but further study is warranted when high-Z lifetime measurements become available.

ACKNOWLEDGMENTS

This work was supported by the Chemical Sciences, Geosciences, and Biosciences Division, Office of Basic Energy Sciences, Office of Science, U.S. Department of Energy, under Grant Nos. DE-FG02-94ER11461 and DE-FG02-97ER14761.

[1] L. J. Curtis and D. G. Ellis, J. Phys. B **29**, 645 (1996).
[2] L. J. Curtis, Phys. Scr. **43**, 137 (1991).
[3] E. Träbert and L. J. Curtis, Phys. Scr. **48**, 586 (1993).
[4] L. J. Curtis, J. Phys. B **26**, L589 (1993).
[5] M. Henderson and L. J. Curtis, J. Phys. B **29**, L629 (1996).
[6] F. Parpia, C. Froese Fischer, and I. P. Grant, Comput. Phys. Commun. **94**, 249 (1996).
[7] E. U. Condon and G. H. Shortley, *The Theory of Atomic Spectra* (Cambridge University Press, Cambridge, 1935) (footnote on pp. 273 and 274).
[8] L. J. Curtis, Phys. Rev. A **40**, 6958 (1989).
[9] L. J. Curtis, Phys. Scr. **62**, 31 (2000).
[10] H. Wolfe, Phys. Rev. **41**, 443 (1932).
[11] G. W. King and J. H. Van Vleck, Phys. Rev. **56**, 464 (1939).
[12] L. J. Curtis, Phys. Scr. (to be published).
[13] L. J. Curtis, D. G. Ellis, and I. Martinson, Phys. Rev. A **51**, 251 (1995).
[14] L. J. Curtis, J. Opt. Soc. Am. B **3**, 177 (1986); **5**, 2399 (1988).
[15] E. Biémont, C. Froese Fischer, M. Godefroid, P. Palmeri, and P. Quinet, Phys. Rev. A **62**, 032512 (2000).
[16] V. Kaufman and J. Sugar, J. Opt. Soc. Am. B **12**, 1919 (1987).
[17] A. Lurio and R. Novick, Phys. Rev. A **134**, A608 (1964).
[18] F. W. Byron, M. N. McDermott, and R. Novick, Phys. Rev. A **134**, A615 (1964).
[19] W. Ansbacher, E. H. Pinnington, J. A. Kernahan, and R. N. Gosselin, Can. J. Phys. **64**, 1365 (1986).
[20] E. Peik, G. Hollemann, and H. Walther, Phys. Rev. A **49**, 402 (1994).
[21] E. H. Pinnington, J. A. Kernahan, and W. Ansbacher, Can. J. Phys. **65**, 7 (1987).
[22] E. H. Pinnington, W. Ansbacher, J. A. Kernahan, R. N. Gosselin, J. L. Bahr, and A. S. Inamdar, J. Opt. Soc. Am. B **2**, 1653 (1985).
[23] E. H. Pinnington, W. Ansbacher, and J. A. Kernahan, J. Opt. Soc. Am. B **4**, 696 (1987).
[24] E. H. Pinnington, W. Ansbacher, J. A. Kernahan, and A. S. Inamdar, J. Opt. Soc. Am. B **2**, 331 (1985).
[25] W. Ansbacher, E. H. Pinnington, A. Tauheed, and J. A. Kernahan, J. Phys. B **24**, 587 (1991).
[26] J. A. O'Neill, E. H. Pinnington, K. E. Donnelly, and R. L. Brooks, Phys. Scr. **20**, 60 (1979).
[27] J. A. Kernahan, E. H. Pinnington, J. A. O'Neill, J. L. Bahr, and K. E. Donnelly, J. Opt. Soc. Am. **70**, 1126 (1980).
[28] L. J. Curtis, H. G. Berry, and J. Bromander, Phys. Lett. A **34**, 169 (1971).
[29] L. J. Curtis, in *Beam Foil Spectroscopy*, edited by S. Bashkin (Springer, Berlin, 1976), pp. 63–109.
[30] T. Andersen, A. Kirkegård Nielsen, and G. Sørensen, Phys. Scr. **6**, 122 (1972).
[31] T. Andersen and G. Sørensen, Phys. Rev. A **5**, 2447 (1972).
[32] T. Andersen and G. Sørensen, J. Quant. Spectrosc. Radiat. Transf. **13**, 369 (1973).